The Forward Time Projection Chamber (FTPC) in STAR

K.H. Ackermann[5], F. Bieser[4], F.P. Brady[2], D. Cebra[2], J.E. Draper[2], V. Eckardt[5], T. Eggert[5], H. Fessler[5], K.J. Foley[1], V. Ghazikhanian[3], T.J. Hallman[1], M. Heffner[2], H. Hümmler[5], J. Klay[2], S.R. Klein[4], A. Lebedev[1], M.J. LeVine[1], T. Ljubicic[1], G. Lo Curto[5], R.S. Longacre[1], M. Oldenburg[5], HG. Ritter[4], J.L. Romero[2], N. Schmitz[5], A. Schüttauf[5], J. Seyboth[5], P. Seyboth[5], M. Vidal[5], C. Whitten Jr. [3], E. Yamamoto[3]

[1] *Brookhaven National Laboratory, Upton, New York 11973, USA*
[2] *University of California, Davis, California 95616, USA*
[3] *University of California, Los Angeles, California 90095, USA*
[4] *Lawrence Berkeley National Laboratory, Berkeley, California 94720, USA*
[5] *Max-Planck-Institut für Physik, 80805 München, Germany*

Abstract

Two cylindrical forward TPC detectors are described which were constructed to extend the phase space coverage of the STAR experiment to the region $2.5 < |\eta| < 4.0$. For optimal use of the available space and in order to cope with the high track density of central Au+Au collisions at RHIC, a novel design was developed using radial drift in a low diffusion gas. From prototype measurements a 2-track resolution of 1 - 2 mm is expected.

1 Introduction

The Forward Time Projection Chambers (FTPC) were constructed to extend the acceptance of the STAR experiment [1]. They cover the pseudorapidity range of $2.5 < |\eta| < 4.0$ on both sides of STAR and measure momenta and production rates of positively and negatively charged particles as well as of neutral strange particles. Due to the high multiplicity, approximately 1000 charged particles in a central Au+Au collision, also event-by-event observables like $\langle p_T \rangle$, fluctuations of charged particle multiplicity and collective flow anisotropies can be studied. The increased acceptance improves the general event characterization in STAR and allows the study of asymmetric systems like p+A collisions. The design and construction was carried out by the group from MPI Munich with contributions from LBNL Berkeley, BNL Brookhaven, UC Davis, UCLA Los Angeles, and MEPhI Moscow [1,2].

2 Detector Design

2.1 Conceptual Design

The FTPC concept was determined mainly by two considerations: Firstly by the high particle density with tracks under small angles with respect to the beam direction and secondly by the restricted available space inside the TPC [3], where the FTPCs are located. In Fig. 1 the final design is shown. It is a cylindrical structure, 75 cm in diameter and 120 cm long, with a radial drift field and readout chambers located in 5 rings on the outer cylinder surface. Each ring has two padrows and is subdivided azimuthally into 6 readout chambers. The radial drift configuration was chosen to improve the two-track separation in the region close to the beam pipe where the particle density is highest. The field cage is formed by the inner HV-electrode, a thin metalized plastic tube, and the outer cylinder wall at ground potential. The field region at both ends is closed by a planar structure of concentric rings, made of thin aluminum pipes. The front end electronics (FEE), which amplifies, shapes, and digitizes the signals, is mounted on the back of the readout chambers. Each particle trajectory is sampled up to 10 times. The ionization electrons are drifted to the anode sense wires and induced signals on the adjacent cathode surface are read out by 9600 pads (each 1.6×20 mm^2). The above design has some unusual and new features for a TPC:

- The electrons drift in a radial electrical field perpendicular to the solenoidal magnetic field.
- Curved readout chambers are used to keep the radial field as ideal as possible.
- A two-track separation of 1-2 mm is expected, which is an order of magnitude better than in all previously built TPCs with pad readout.

To meet these requirements a R+D program was initiated, including the selection of the most suitable gas mixture, the development of the fabrication technology for the curved readout chambers, and the optimization of the wire and pad geometry for the readout chambers.

2.2 Selection of Gas Mixture

Due to the short drift length of only 23 cm a cool gas mixture with CO_2 or DME can be used. It has a low diffusion coefficient for electrons and a small Lorentz angle [4]. After extensive measurements an Ar/CO_2 ($50\%/50\%$) mixture was selected which is non-flammable, shows no or little ageing effect in comparison to hydrocarbons and is chemically less agressive than a mixture with DME. Fig. 2 shows the measurements of drift time, cluster sizes, deflection angle due to the Lorentz force in the magnetic field and two track resolution for the Ar/CO_2 gas mixture [1].

2.3 Readout Chambers

In a conventional TPC the anode (amplification) wires are orthogonal to

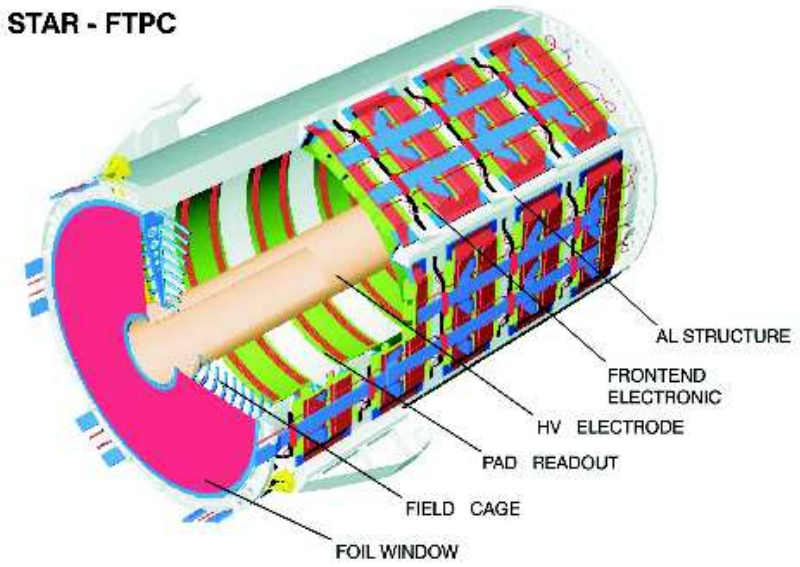

Fig. 1. Schematic diagram of an FTPC for the STAR experiment

the axial direction of the pads. This is impossible in the case of a curved readout chamber. The wires can not be parallel to the pads and therefore to the cylinder axis either, because focusing effects then lead to periodic shifts in the position measurement. This is demonstrated in fig. 3. However, if two or more wires cross the pad under a small angle this effect already vanishes. For the FTPC design an angle of 17.4^0 was chosen resulting in three wires crossing each pad for the selected pad-wire geometry. The anode wires are first glued on the flat pad plate with conductive epoxy. Afterwards the plate is bent between 3 rollers to the final curvature without breaking the wires. A complete readout chamber with 2 padrows is shown in fig. 4. With only 1.5 mm distance between the anode wires and the pad plane the spread of the signal (the so-called Pad Response Function) is of similar narrow width. This together with the low electron diffusion and the radial drift principle results in the required 2-track separation of about 1 mm as can be seen in fig. 5.

2.4 Readout Electronics

The two FTPCs have 19.200 channels of electronics, capable of measuring the charge drifting to the readout chambers in short time samples. The drift time of about 50 μs for the 23 cm maximum drift length is subdivided into 256 time bins. Because of the slow drift gas and the resulting long duration of the collection of the electron cloud from a track crossing a shaping time of 350 ns is used. The sampling

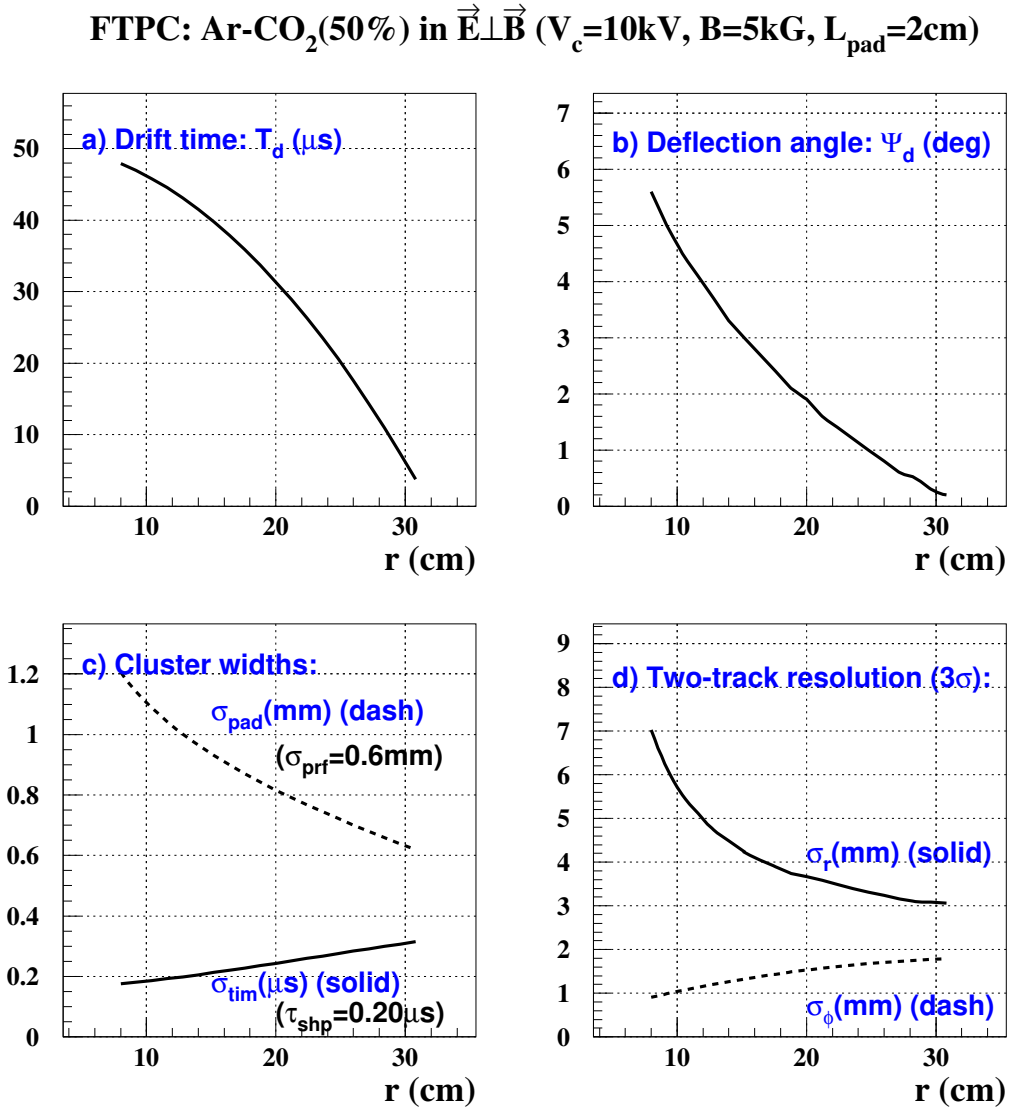

Fig. 2. Electron cluster properties as a function of the radial position of the track hit in the FTPC. (a) drift time; (b) deflection angle; (c) cluster widths in time (μs, solid line) and pad (mm, dashed line) directions; (d) two-track resolution (3σ) in the radial (solid line) and azimuthal (dashed line) directions.

rate is 5 MHz. The design of the front end electronics closely follows that of the central TPC [5]. Each pad is read out by a low-noise STAR preamplifier/shaper (SAS), which sends signals to a switched capacitor array/ADC chip (SCA/ADC). Four of these chip sets, handling 64 channels, are mounted on a small FEE card, which is positioned directly on the detector, parallel to the readout chambers. Fifteen FEE cards are read out by a readout board, which sends the signals via a 1.2 Gbit/s fiber-optic link to the data acquisition system. The readout board also controls the FEE cards, utilising signals from the clock and trigger distribution system, and the slow control

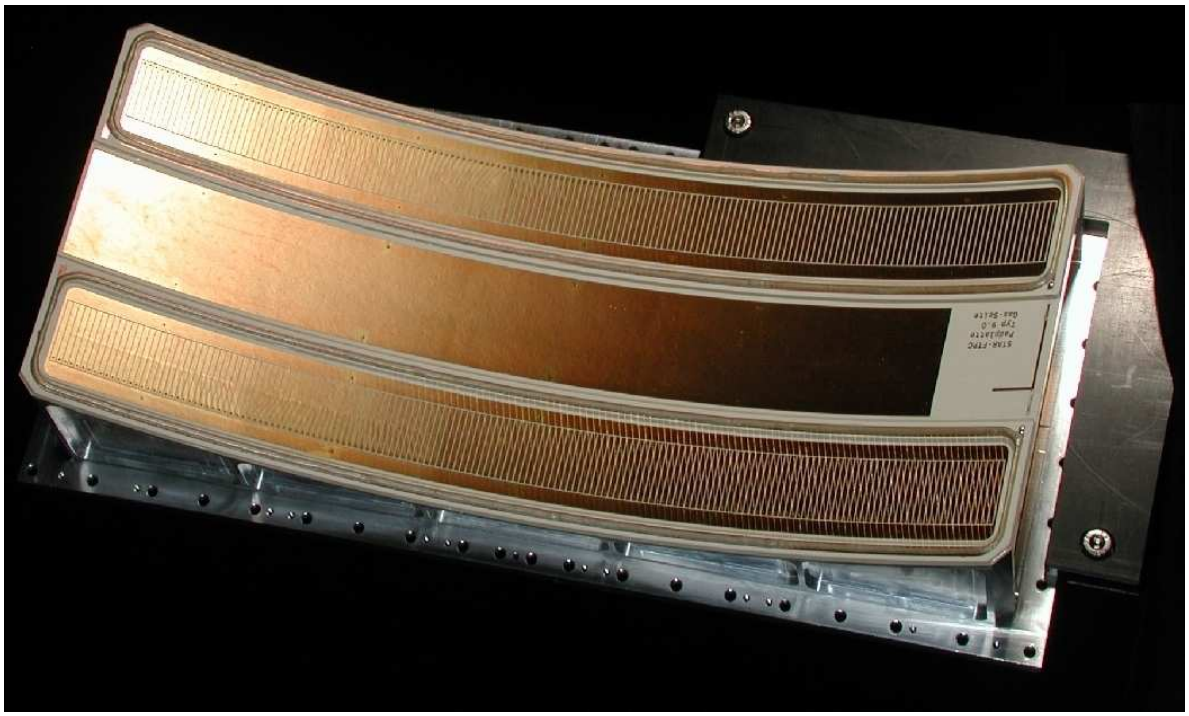

Fig. 4. Photograph of a FTPC readout chamber. The bending radius is 305 mm and each of the two padrows has 160 pads.

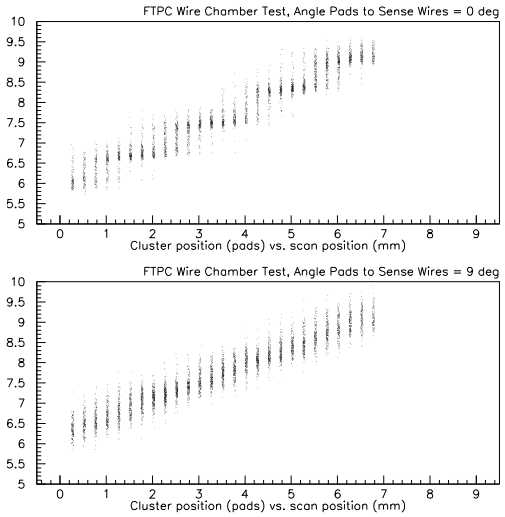

Fig. 3. Measured position of a laser beam for two crossing angles between the anode wires and the pad axis. For 0^o (top) systematic shifts due to the wire structure are observed, which disappear for 9^o angle (bottom).

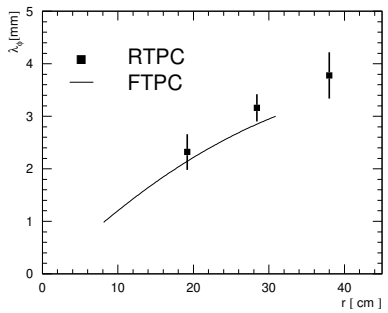

Fig. 5. Measured 2-track resolution in the prototype RTPC (data points) and expected reolution in the FTPC (line) as a function of the radial distance r from the beam axis.

links. For maintaining the proper operating temperature the FEE and readout boards are water cooled using a leakless, low pressure circulation system [9]. The FTPCs are remotely operated through a VME based supervision system. Data logging and visualisation are performed by a software package developed within the EPICS mainframe [10].

2.5 Laser Calibration System

The laser calibration system serves three primary purposes:

- Providing straight tracks of known position to infer corrections for spatial distortions due to mechanical or drift field imperfections.
- Helping to calibrate the drift velocity in the nonuniform radial drift field.
- Allowing detector testing independent from collider operation.

The primary laser beams are produced by Nd:YAG lasers, run in the fourth harmonic (266 nm), which are also used by the STAR-TPC laser system [6]. These beams with 30 mm diameter are transported to the FTPCs, one on each side. Two remote controlled mirrors in each transfer path and two CCD cameras allow precise steering of the beam toward the detector. A distribution box subdivides the incoming beam into three beams with 8 mm diameter each. Two 45^0 mirrors bring the smaller beams to fused silica windows in the gas containment wall. Inside the FTPC they hit five 1 mm pickoff mirrors mounted on a 5 mm ceramic tube at different radial positions. The five beams are arranged in a plane with three beams parallel to the detector axis and two tilted to allow measurements at many radii. The three planes are displaced by approximately 120^0 in azimuth.

3 Simulation and Reconstruction of Experimental Data

The first step in the reconstruction of tracks is to calculate the track points (cluster finding) from the charge distribution measured by the readout electronics. In a second step (track finding), these track points are grouped to tracks. Using the magnetic field map, the up to ten position measurements per track are then used to fit the momentum.

3.1 Cluster Finding

The reconstruction of track points is done by the FTPC cluster finding program [7]. It is optimized to deal with high track densities while minimizing the use of computing time. The program reads in the electronic signal data from the data acquisition system, looks for areas of nonzero charge (cluster), deconvolutes clusters and fits the point coordinates. The transformation from pad position and drift time into cartesian coordinates includes the correction of distortions introduced by the magnetic field. For a typical central Au+Au collision with 1000 particles in both FTPCs and an occupancy of 25% in the inner region the program needs about 2 seconds on a 930 MHz Intel PentiumII processor.

3.2 Track Reconstruction

The second step in the analysis of FTPC data is the reconstruction of the particle tracks and their momenta. The FTPC track reconstruction code

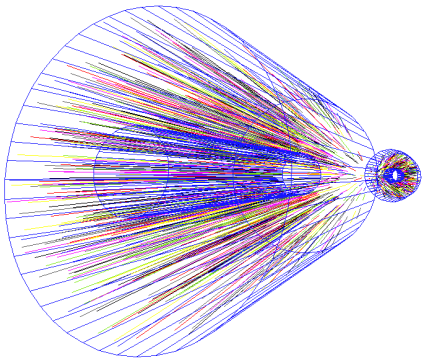

Fig. 6. Reconstructed tracks in the FTPCs from a Au+Au collision at $\sqrt{s_{NN}} = 200$ GeV simulated with the HIJING model. From 14.745 space points 1.026 tracks were reconstructed.

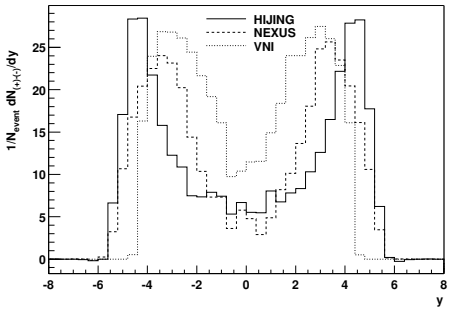

Fig. 7. Rapidity distribution of net positive charges (excess of positively over negatively charged particles) in Au+Au collisions at $\sqrt{s_{NN}}$ = 200 GeV simulated with three different models.

is based on an algorithm developed for fast online reconstruction [8]. It is a conventional track-following algorithm optimized for minimum use of computing power. In this code all position calculations are done in a transformed coordinate system in which points appear on a straight line if they form a helix in cartesian coordinates. This processing step is known as conformal mapping [8]. It saves calculation time in the track fitting, because all fits can be done by linear regression. After the track finding step the code determines a primary vertex position by extrapolating and intersecting all the reconstructed tracks. Finally the particle momenta are fitted using the magnetic field map and the vertex position. Fig. 6 shows a reconstructed HIJING event for a central Au+Au collision at 200 GeV per nucleon pair. From 14.745 space points 1026 particle tracks were reconstructed in less than 2 seconds.

4 Physics Simulation Studies

Simulation studies demonstrate the capability of distinguishing different theoretical models of nucleus-nucleus collisions such as HIJING, NEXUS and VNI with measurements in the FTPCs. Fig. 7 shows the rapidity distribution of net positive charges which follow the p - $\bar{\mathrm{p}}$ distribution and characterise the baryon stopping in the reaction. Fig. 8 shows histograms of the effective temperature as determined event-by-event. Such measurements will be used to study and search for fluctuations of event properties and to select special event classes.

5 Summary

Based on the prototype measurements and simulations one expects to obtain a position resolution of 100 μm, a two-track-separation of 1mm, a momentum resolution between 12 and 15 $\%$, and an overall reconstruction efficiency between 70 and 80 $\%$.

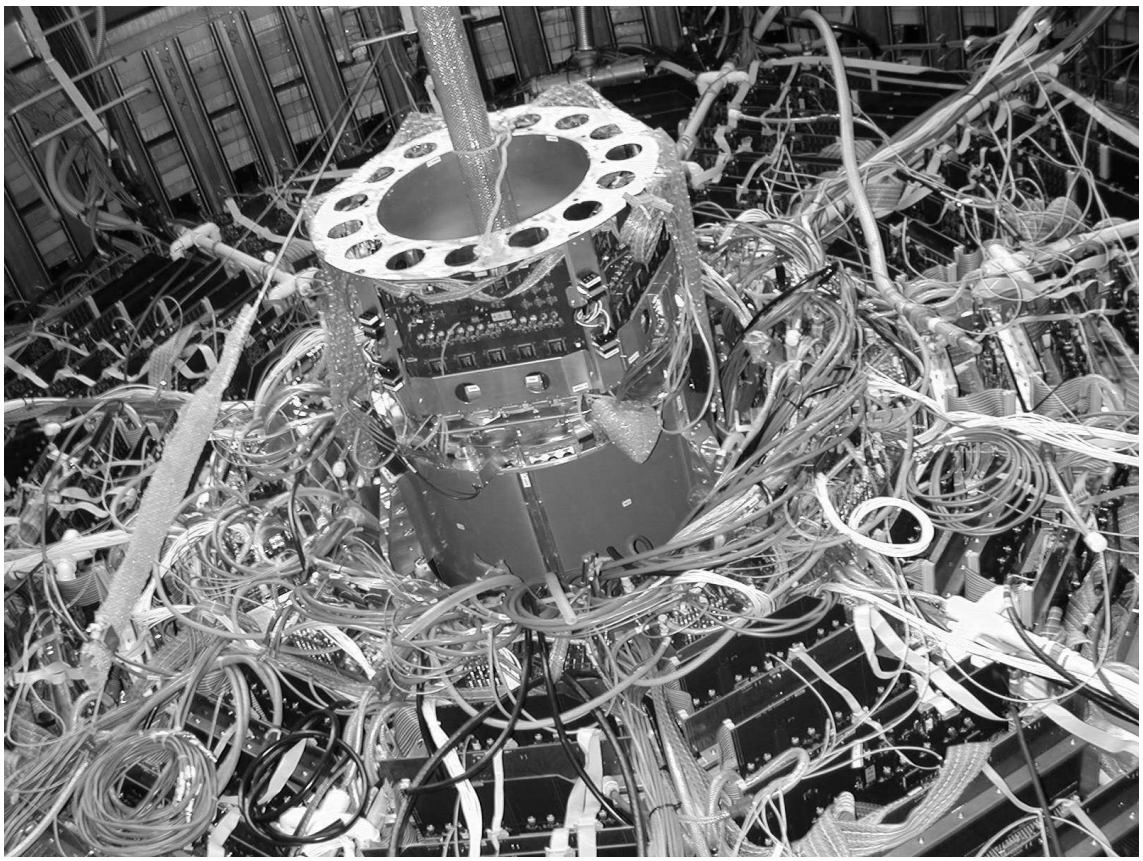

Fig. 9. One FTPC installed inside the STAR detector

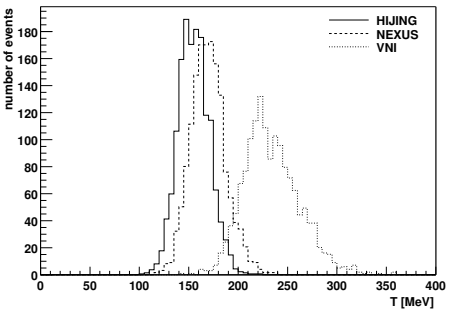

Fig. 8. Distributions of the temperature parameter T reconstructed event-by-event in the FTPCs for three different event generators.

A summary of the main characteristics of the FTPCs is given in table 1. The completed and tested FTPCs have been installed in the STAR experiment for first data taking during summer and fall of 2001. One of them can be seen mounted inside the STAR detector in Fig. 9.

Table 1
FTPC parameters

PARAMETER	VALUE
Configuration	
# of TPC	2
rows per TPC	10
sectors per pad row	6
pads per sector	2×160
Sensitive Volume	
inner radius	8.0 cm
outer radius	30.5 cm
chamber length	120.0 cm ($150 < \|z\| < 270$ cm)
acceptance	$2.5 < \|\eta\| < 4.0 (2.0^o < \theta < 9.3^o)$
Field Cage	
drift cathode voltage	10-15 kV
drift electrical field	240-1400 V/cm (radial)
solenoid magnetic field	0.5 T
Gas	
gas mixture	Ar(50%)-CO_2(50%)
drift velocity	0.3 - 2.0 cm/μs
trans. diffusion D_T	100-130 μm/$\sqrt{cm}$
long. diffusion D_L	100-130 μm/$\sqrt{\mathrm{cm}}$
Lorentz angle	4 deg. (at 0.5 T)
gas gain	$\sim$ 1-2$\times 10^3$
Readout	
# of pads	19200
time bins per pad	256
pad pitch	1.9 mm
pad length	20 mm
anodewire–pad gap	1.5 mm
shaping time (FWHM)	350 ns
SCA time bin size	218 ns
ADC dynamic range	10 bits

References

[1] F. Bieser et al., The Forward Time Projection Chamber for the STAR Detector, *MPI PhE/98-3*, 1998

[2] A. Schüttauf et al., A Forward TPC for STAR, *Nucl. Phys.* **A 661** (1999) 677c

[3] H. Wieman et al., STAR TPC at RHIC, *IEEE Trans. Nucl. Sci.* **44** (1997) 671

[4] X. Bittl et al., Diffusion and Drift Studies of Ar-DME/CO_2/CH_4 Gas Mixtures for a radial TPC in the E$\times$B Field, *Nucl. Instr. Meth.* **A 398** (1997) 249

[5] S. Klein et al., Front-End Electronics for the STAR TPC, *IEEE Trans. Nucl. Sci.* **43** (1996) 1768

[6] M. Alyushin et al., Laser Calibaration System for STAR TPC, *IEEE Nucl. Sc. Symp. Conference Record* **96CH35974** (1996),
Proceedings of the 9th Vienna Conference on Intrumentation, *Nucl. Instr. Meth.* in print

[7] H. Hümmler, Doctorate Thesis, Technical University, München, Germany, 2000, *MPI PhE/2001-04* 2001,
H. Hümmler, Simulation and Reconstruction of Data from the STAR FTPC, *STAR Note SN0429* (2000)

[8] P. Yepes, A fast track pattern recognition, *Nucl. Instr. Meth.* **A 380** (1996) 582
M.Oldenburg, Doctorate Thesis, Technical University, München, Germany, 2001, in preparation

[9] M. Bosteels, Cern internal report, CERN/LHCC/99-33 (1999)

[10] A.J. Kozubal et al., ICALEPS89 Proceedings, 288, (Vancouver, 1989)